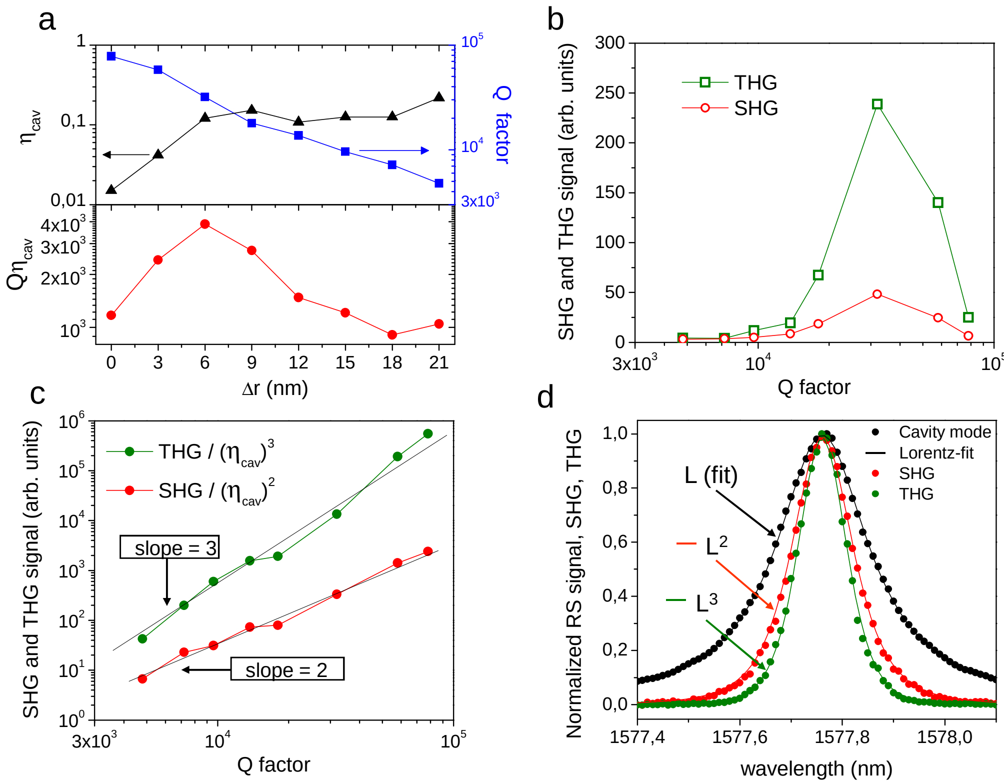

Fig. 5. Q-factor and lineshape scalings. (a) Upper panel, Q-factor (right axis) and corresponding coupling efficiency η_{cav} (left axis) of the far-field modified PhC nanocavities as a function of the holes enlargement Δr. Lower panel, the product $Q\eta_{cav}$. (b) SHG and THG emission intensity vs. Q-factor for the same series of PhC cavities. The HG signals peak around $Q \sim 3 \times 10^4$, which corresponds to the cavity with $\Delta r = 6$ nm in (a) that has the highest $Q\eta_{cav}$ product. (c) Normalized SHG and THG emission intensity (see text) as a function of the cavity Q factor showing clear Q^2 and Q^3 scaling, respectively. (d) Resonant scattering spectrum of a PhC nanocavity with $Q = 5.2 \times 10^3$ (black dots), and best-fit to a Lorentzian lineshape (black line, L). SHG and THG spectra recorded while scanning the pump laser across the cavity resonance (red and green dots, respectively). Red and green lines interpolating the SHG and THG data are the squared (L^2) and cubed (L^3) Lorentzians, respectively.

nanocavities to enhance optical nonlinearities, we demonstrate an impressive improvement in THG efficiency of more than 10 orders of magnitude and a reduction in pump power by 6 orders of magnitude.

6. Discussion and conclusions

Despite the onset of saturation in the HG signal occurring for high-Q PhC cavities, our experiments represent a considerable improvement over previous works on silicon [30–33], since HG light is observed here under a continuous-wave pumping regime. This is quite unexpected due to the presence of strong TPA and consequent free-carrier absorption in silicon - the same parasitic effect that prevents cw Raman lasing in Si devices unless a free-carrier lifetime reduction mechanism is applied [15]. We demonstrate here that efficient continuous-wave HG is possible in a silicon nanodevice, thus making the major step towards possible widespread applications. Moreover, we note that the pump power required to observe efficient emission is ten times lower than that for a recently demonstrated microlaser [51], which highlights the surprising fact that light sources based on HG emission may be more efficient than lasers.

Even though at present the maximum observed THG power may be considered still low for immediate applications in signal processing devices, the conversion efficiency of our device can be further increased in several ways: 1) by increasing the $Q\eta_{cav}$ product, i.e. by designing PhC nanocavities with higher Q-factor and coupling efficiency, while keeping a comparable mode volume; 2) through polarization of the device with a p-n junction to sweep-out free-carriers from the cavity region, i.e. as in Raman laser devices [15]; 3) by the introduction of carrier-recombination centers through controlled ion-implantation [52]. The combined application of these strategies is expected to increase substantially the emission efficiency by 2-3 orders of magnitude, thus bringing the blue-THG output power of our Si nanocavity to a level that is comparable to the highest reported ($\sim$ 500 pW) red-SHG power in a III-V-based nanodevice [28].

In the present geometry the pump electromagnetic field is in-coupled through far-field optimization out of the plane. We point out that an alternative integrated signal-processing device could be realized by pumping the cavity through a side-coupled PhC waveguide in a geometrical configuration already reported [20]. This would lead, for instance, to a channel-drop device where infrared signals could be injected on-chip and ”dropped” out-of-plane at visible wavelengths. On the other hand, achieving a full on-chip device for both pump and harmonic signals would require to suppress absorption, i.e., to change the PhC slab material in order to have transparency also at the harmonic frequency.

In conclusion, we have presented the first demonstration of nonlinear frequency conversion by simultaneous SHG and THG in silicon PhC nanocavities using low-power continuous-wave light. We achieved efficient dual wavelength emission in the blue/green and red visible windows with excitation in the telecom bands and with a few tens of microwatts power. The low-power continuous-wave operation, wide tunability and full CMOS compatibility of our silicon nano-emitter are important features which add considerable weight to the opportunity of making silicon a truly pervasive material for Photonics.

Acknowledgments

The authors would like to acknowledge D. Bajoni and M. Liscidini for useful discussions and S. L. Portalupi, M. Spurny, S. Balfour and G. Robb for help with experiments. This work was partly supported by Era-NET NanoSci LECSIN project coordinated by F. Priolo, and by Italian Ministry of University and Research, FIRB contract no. RBAP06L4S5. Fabrication was carried out in the framework of NanoPIX (www.nanophotonics.eu).

#136479 - $15.00 USD Received 12 Oct 2010; revised 19 Nov 2010; accepted 21 Nov 2010; published 3 Dec 2010